IEEE Access
Multidisciplinary | Rapid Review | Open Access Journal

SPECIAL SECTION ON SMART CACHING, COMMUNICATIONS, COMPUTING AND CYBERSECURITY FOR INFORMATION-CENTRIC INTERNET OF THINGS

Received May 15, 2019, accepted June 8, 2019, date of publication June 20, 2019, date of current version July 22, 2019.

Digital Object Identifier 10.1109/ACCESS.2019.2924202

Design of MIMO-Visible Light Communication Transceiver Using Maximum Rank Distance Codes

ARSLAN KHALID[1], HAFIZ M. ASIF[2], SHAHID MUMTAZ[3], SATTAM AL OTAIBI[2], AND KOSTROMITIN KONSTANTIN[4]

[1]Department of Electrical Engineering, The University of Lahore, Lahore 54000, Pakistan
[2]Department of Electrical Engineering, Taif University, Ta'if 26571, Saudi Arabia
[3]Instituto de Telecomunicações, 3810078 Aveiro, Portugal
[4]Department of Physics of Nanoscale Systems, South Ural State University, 454080 Chelyabinsk, Russia

Corresponding author: Hafiz M. Asif (hafizasif@ciitlahore.edu.pk)

This work was supported by Taif University.

ABSTRACT This paper is aimed at comparing the performance of multiple-input multiple-output (MIMO) schemes applied to the indoor visible light communication (VLC) system. The MIMO schemes considered for this paper are repetition coding (RC), space-time block codes (STBCs), and spatial multiplexing (SMP). For MIMO design, the current system makes use of unique algebraic codes, i.e., maximum rank distance (MRD) codes in this connection. Two different configurations (2×1 and 2×2) are taken into consideration with distinct transmitters' spacing. Simulation results are presented and a comparative analysis of the current system with an existing system is given mainly in terms of bit error rate (BER), data-rate, and transmission range. The simulation results are validated by the physical implementation of the system using NI cDAQ module programmed in LabVIEW. The simulation and experimentation results indicate that the RC scheme with significant diversity gain provides more robustness as compared to other MIMO schemes; however, the RC exhibits poor multiplexing gain, and hence, it is not spectral efficient. As its counterpart, the STBC and SMP are used that can increase both the capacity and reliability at the cost of slightly reduced transmission range.

INDEX TERMS Line of sight (LOS), light emitting diode (LED), modified space-time block codes (MSTBC), maximum rank distance codes (MRD), repetition coding (RC), software-defined radio (SDR), spatial multiplexing (SMP), visible light communication (VLC), zero-forcing detector (ZF).

I. INTRODUCTION

The ongoing user demands for high-speed wireless broadband home access networks are frequently increasing and it is getting difficult for radio frequency (RF) based wireless system to accommodate all user requirements. The RF spectrum has already gridlock and therefore, looking for alternative technologies could be the way forward. In this connection, Optical Wireless Communication (OWC) system has become one of the emergent and the cost-effective technologies that employ mono-chromatic light to transmit the digital data via intensity-modulation and direct-detection (IM/DD) optical wireless channel [1]–[5]. In IM/DD, the information bits are transmitted in the form of intensity or power of light. As a result, phase information is not required for communication. While on the receiver side, the intensity or power of an optical signal is directly detected.

The associate editor coordinating the review of this manuscript and approving it for publication was Jun Wu.

As a light source, the OWC system relies on recently developed LEDs that eventually substitute conventional lighting devices. By integrating LEDs (that emits light in the visible light spectrum) with a communication system, there exists a Visible Light Communication (VLC) system that has several unique features such as interference-free spectrum (384 THz – 789 THz), high transmission speed, dual use (illumination and high speed data communication), ubiquitous, secure as light signals fail to pass through the walls, low cost opto-electronic components, stable channel conditions for the specific symbol duration, high signal-to-noise ratio (SNR) and harmless for the human body [3], [6], [7].

A. PRIOR WORKS

Despite several myriad VLC features, there still exits some challenges such as the design of duplex transmission system, the dimming control, and achieving high data-rates which are constrained by low modulation bandwidth of LED [6].

The problem of duplex transmission was targeted in [8]–[10] while several works have also been done on dimming control [11]–[13]. The ongoing research activities are done on improving both capacity and reliability of VLC systems. For this, significant amount of work can be seen in which more advanced spectral efficient modulation techniques such as Orthogonal Frequency-Division Multiplexing (OFDM) [14], [15] and its variant such as asymmetrically-clipped optical OFDM (ACO-OFDM) [16], [17], DC-biased optical OFDM (DCO-OFDM) [18] and asymmetrically-clipped DC-biased optical OFDM (ADO-OFDM) are implemented [16]. For the case of IM/DD, the output of OFDM and its variant should be positive and real. In order to do so, generally, Hermitian symmetry (HS) block is introduced to the OFDM system before carrying out the inverse fast Fourier transform (IFFT) operation. The HS increases the computational complexity of the transceiver as the block size of IFFT and FFT becomes double. In the meantime, HS also put a limit on the capacity of the VLC system as the only half sub-carriers are accustomed to transfer the data [19]. Furthermore, it was also shown in [20]–[22] that the OFDM gives high peak-to-average-power-ratio (PAPR) and for the real-valued non-negative envelope, a changeable LED driver circuit is desirable which is complex to build and very expensive. So, our earlier work [23] target the issues of OFDM and suggested modified form of OFDM named as Enhanced Sub-carrier Index Modulation OFDM (ESIM-OFDM) and an appropriate signal shaper such as Sigma-Delta Modulator (SDM). ESIM-OFDM tackles the issue of high PAPR of OFDM while SDM converts the real-valued signal to square waveform so as to be used for data communication through LEDs. However, it was observed through hardware-based numerical results shown in [23] that SDM reduces data-rate and increases the computational complexity of the VLC system.

In lieu of OFDM techniques, multiple-input multiple-output (MIMO) techniques have also been viewed as the most promising in achieving high data-rates and improving reliability. The MIMO systems exploit the property of multiple LEDs installed on a ceiling of a room that provides sufficient illumination as well as data communication. Recently, many investigators have suggested MIMO-VLC systems based on Space-Time Block Codes (STBCs) [24]–[27], Spatial Multiplexing (SMP) [28], [29] and Repetition Codes (RC) [30]–[32]. The most interesting feature of using both RC and STBCs in VLC system is that they can enhance the reliability without increasing the transmitting optical power. However, additional processing is required at the receiving end. In the meantime, SMP is used to enhance the capacity of the system.

The RC, with on-off keying (OOK) and pulse-position modulation (PPM), was first introduced in [33] and [34] in which the same binary signal was transmitted by two spatially separated VLC transmitters. Both of these works illustrate the significant amount of diversity gain which was, unfortunately, could not be received in the RF system. This diversity gain is due to the fact that RC combines both faded signals at the single photo-diode before the noise addition. In [28], Cuiwei *et al.* suggested an ACO-OFDM based SMP technique for MIMO systems. Their proposal achieve significant coding gain as well as high data-rate. After some time, Fath *et al.* investigate and analyze the performance of Pulse Amplitude Modulation (PAM) based SMP scheme. However, the authors of both works cannot implement their work on hardware tools.

Later, efforts were made to use STBCs within VLC system that can also provide reliability. However, initial efforts were failed as STBCs employs phase modulation (PSK and QAM) which are not suitable for IM/DD. In this connection, Simon *et al.* proposed a modified STBC system in which BPSK modulated Alamouti blocks were converted to unipolar blocks. The work of Simon et. al was further extended to any number of transmit antennas by Safari and Uysal [31]. However, a very important point can be deduced from their work that by modification, the error performance of the Alamouti blocks deteriorates as they lose orthogonality between the columns. So, there is a great potential to search for a better block code that provides the unipolar output suitable for IM/DD.

B. CONTRIBUTION

All the works reported in the previous subsection only provide the numerical performance analysis and none of the authors have implemented their work on hardware. However, this work provides both numerical performance analysis and hardware implementation of the RC, SMP, and STBCs based VLC system. The work presents a novel technique in the form of algebraic codes i.e., Maximum Rank Distance (MRD) codes which eliminate the need for modification in Alamouti codes. Thereby, producing the unipolar outcome which is the requirement of IM/DD. The feasibility of the proposed system has also been tested through a prototype implementation. The implementation consists of a Software Defined Radio (SDR) based on NI cDAQ component tools designed in MATLAB/LabVIEW. The performance of the designed prototype has been accomplished in relation to transmission range and data-rate mainly. The key contributions are:

- Design VLC transceiver based on algebraic codes (rank codes) and assess the error performance mainly on Bit-Error-Rate (BER) of RC, SMP, and STBCs for numerous transmitters spacing
- Develop a prototype design of VLC transceiver using NI hardware and demonstrate the text communication through it
- Assess the effectiveness of the prototype by computing the transmission range and data-rate for RC, SMP, and STBCs based MIMO system for different configurations (2×1 & 2×2)

C. PAPER ORGANIZATION

The rest of the paper is structured into the following sections: Section II provides a comprehensive explanation of the MIMO system model. Afterward, Section III gives a brief discussion on the RC and SMP. It also provides essen-

tial knowledge for the construction of modified STBC and MRD-STBCs. Section IV discusses and presents the outcome of simulations for 2×1 and 2×2 antenna configuration whereas section V gives details about the experimental setup while the last section gives concluding remarks of the work.

II. SYSTEM MODEL

In this work, an IM/DD based optical MIMO communication system is realized with the help of M_T LED transmitters and M_R receivers (photo-diodes). The received signal vector r is expressed as:

$$r = H_O d + w \tag{1}$$

where w denotes the noise vector which is the sum of thermal and shot noise. It is to be noted that w is a real-valued additive-white Gaussian noise (AWGN) with zero mean and variance $\sigma^2 = \sigma^2_{shot} + \sigma^2_{thermal}$. The original signal transmitted by the emitters is indicated by $d = [d_1\ d_2 \cdots d_{M_T}]^T$. The entries of data vector d show the data symbols transmitted by each transmitter. The optical channel matrix H_O, with $M_R \times M_T$ dimension, is formulated as:

$$H_O = \begin{bmatrix} h_{11} & \cdots & h_{1M_T} \\ \vdots & \ddots & \vdots \\ h_{M_R1} & \cdots & h_{M_RM_T} \end{bmatrix} \tag{2}$$

where $h_{M_RM_T}$ exhibit the transfer factor of an optical link between transmitter M_T and receiver M_R. Optical signals propagate on two distinct paths. The first one is the direct path between the emitter and the receiver, i.e., the line of sight (LOS) path [35]. The other path is not direct and at least dependent on the reflection (and refraction, diffraction, scattering, etc.) of light from different reflecting surfaces present in the indoor environment. This path is called the non line of sight (NLOS) path [36], [37]. For a regular indoor setting, the VLC transmitters are fitted on the ceiling of a room having radiant intensities in the downward direction, whereas the VLC receivers are located at lower heights confronting upwards to the ceiling. Fig. 1 shows the geometry of a cubic room having dimensions $4m \times 4m \times 3m$ and equipped with two transmitters and two receivers. It is worthy to mention that the transmitters are located on the ceiling at the height of $z = 2.50m$ while the receivers are placed at the height of $z = 1m$ on the table. Furthermore, both emitters and receivers are located at the center of the room in an array 2×1. On the basis of a given geometry, numerous static setups will be considered by varying the spacing between the transmitters/receivers. Without any loss of generality, we fix the spacing between the receivers to $0.1m$ while we change the transmitters spacing and investigate their response in the simulation results.

In this study, we only assume LOS path since it carries almost 90% of the total optical power. For LOS link, the channel gain calculations are similar to a single-input single-output (SISO) system. The thorough discussion on LOS link can be seen in [23], [37]–[39]. However, by using

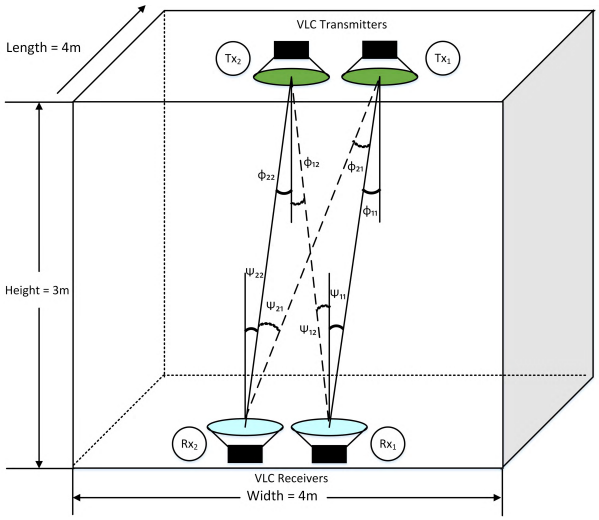

FIGURE 1. Geometry of MIMO-VLC channel in a cubic room.

the given geometry, we present a mathematical expression for the channel gain of optical LOS link as [23], [38]:

$$h = \frac{A_{rx}(k_1 + 1)}{2\pi D^2} \cos^{k_1}(\phi) \cos(\psi) \tag{3}$$

where A_{rx} show the exposure area of photo-diode, D denotes the transmission range, ϕ and ψ illustrates emergence and incidence angle, and k_1 indicates the Lambertian emission parameter which corresponds to emitter's semi-angle at half illuminance $\varphi_{\frac{1}{2}}$. The parameter k_1 is computed as [40]:

$$k_1 = \frac{-ln(2)}{ln(cos\varphi_{\frac{1}{2}})} \tag{4}$$

The Eq. 3 holds true only if incidence angle is comparatively lesser than the field-of-view (ψ_{FOV}). In the case, $\psi > \psi_{FOV}$, the channel gain h is equal to zero. It is worth-telling here that both angles, $\varphi_{\frac{1}{2}}$ and ψ_{FOV} are selected to be 15° as these angles are used in the physical implementation of LOS link in European Union project OMEGA [41].

III. MIMO TECHNIQUES

This section presents a comprehensive discussion of the existing and proposed MIMO techniques used for indoor OWC. For all MIMO schemes, it is presumed that the receivers have perfect channel knowledge and thus employed a zero-forcing linear detector as an equalization technique. Moreover, the emitters and receivers are completely synchronized with each other.

A. REPETITION CODE BASED VLC SYSTEM

For IM/DD, the transmit diversity is simply realized by the RC in which same OOK signal is simultaneously transmitted by the spatially separated M_T transmit antennas. The optical power in RC is uniformly distributed among all the VLC transmitters, thus, the light intensities are divided by the factor M_T. On the receiver side, the light intensities originating from different LED transmitters are constructively adding up

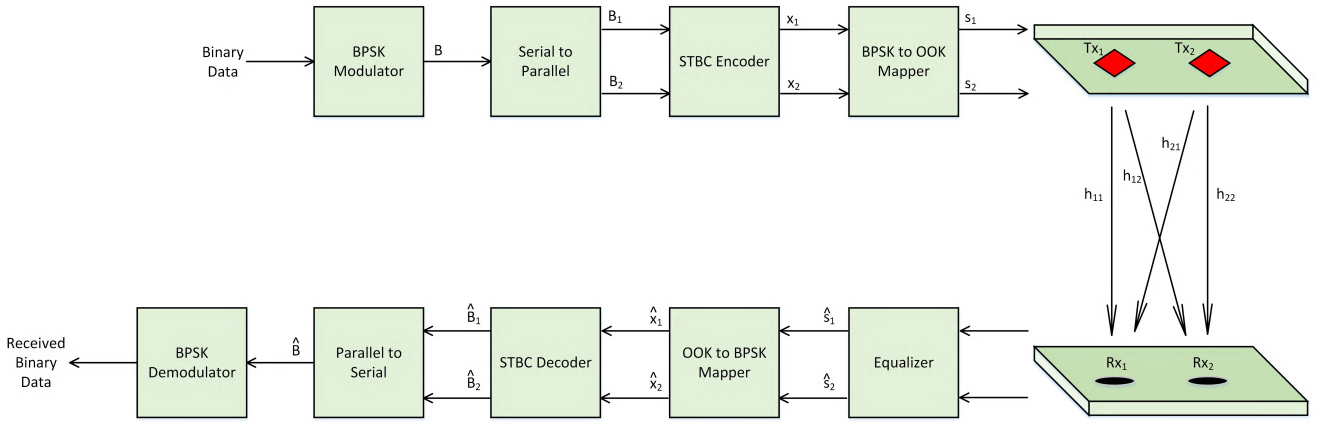

FIGURE 2. Schematic diagram of MSTBC based MIMO-VLC system.

at the single photo-diode [32]. The mathematical expression of the received signal is given as [42]:

$$r_s = \frac{R_p}{M_T} \sum_{a=1}^{M_T} h_a d + w \tag{5}$$

where R_p denotes the responsivity of receiving photo-diode, h_a are the VLC channel dc gain, d are the data symbols and w represents the noise which is modeled as AWGN.

B. SPATIAL MULTIPLEXING BASED VLC SYSTEM

Spatial Multiplexing (SMP) is also a MIMO scheme that is utilized to raise the data-rate of the system. The idea of SMP is the simultaneous transmission of independent data streams via all VLC emitters exist in the setup. The SMP provides the spectral efficiency of $M_T log_2(M)$ bit/s/Hz, where, M signifies the constellation points. In this study, randomly generated binary data is first passed to the OOK modulator. The serial outcome of the modulator is converted into two parallel streams to transmit through VLC transmitters. For the first time-slot, the OOK symbols s_1 and s_2 are relayed through transmitter 1 and 2 respectively. While in the second time-slot the transmitters send s_3 and s_4. Consequently, the system attains spectral efficiency.

C. MODIFIED STBC FOR VLC SYSTEM

The schematic diagram of the modified STBC based MIMO-VLC system is exhibited in Fig. 2. Initially, the binary data from the user is taken and passed to the BPSK modulator. The modulated data B is split up into two sequences (B_1 and B_2) and then passed to the STBC encoder. The output of the STBC encoder contains the phase information as the modulated symbols are $+1$ and -1, therefore, there is a need to make them real and positive. To create the STBC blocks unipolar, a mapper is placed right after the STBC encoder that converts BPSK modulated symbols x_1 and x_2 into unipolar OOK symbols s_1 and s_2. The complete algorithm used by the BPSK to OOK mapper can be found in [31], however, the mathematical expressions used by the mapper are:

$$S = \frac{1_{2\times 2}}{2} + \frac{X}{2} \tag{6}$$

where $1_{2\times 2}$ is a square matrix whose entries are equal to 1s while X is a 2×2 STBC block. As an example, consider a BPSK modulated STBC block as $\begin{bmatrix} 1 & 1 \\ -1 & 1 \end{bmatrix}$. After passing the STBC block through mapper, the unipolar output is given as $\begin{bmatrix} 1 & 1 \\ 0 & 1 \end{bmatrix}$. The resultant unipolar block is termed as modified STBC block and it will be transmitted through a line of sight VLC channel.

On the receiver side, the optical intensities from independent transmitters are detected by the photo-diodes which after optical to electrical convergence passed to ZF equalizer. The equalized OOK symbols ($\hat{s_1}$ and $\hat{s_2}$) is transferred back to BPSK symbols ($\hat{x_1}$ and $\hat{x_2}$) by the transformation:

$$\hat{X} = 2\hat{S} - 1 \tag{7}$$

The output of the demapper is supplied to the STBC decoder that will recover the BPSK symbols. Afterward, the parallel streams are transformed to serial data and enter to the BPSK demodulator. The end result of the demodulator is then compared with the original data to examine the number of errors.

D. MRD-STBC BASED VLC SYSTEM

MRD codes are algebraic codes that are linear in nature and generated using primitive polynomials. A linear code can be represented as $\mathcal{C} = (n, k, d)$, where n relates to the length of the code, k indicates the quantity of symbols and d signifies the code distance. MRD codes are based on metric 'rank' constructed by Gabidulin [43] and Gabidulin and Pilipchuk [44] that attempts to detect and correct more number of errors in comparison with other codes based on metric 'minimum hamming distance' [45]. This error handling capability is due to linear dependency among different symbols.

Let a finite field of p elements will be represented by $\mathbb{F}_p$. This ($\mathbb{F}_p$) field is considered as the base field and its

extension field of M_T is given as $\mathbb{F}_{p^{M_T}}$, where p denotes prime number ($p = 2, 3, 5 \ldots$). Moreover, let $\mathbb{R} = (r_1, r_2, \ldots, r_n)$ be an $n-$vector whose co-ordinates lie in the extension field. Let $m_1, m_2, \ldots, m_{M_T}$ represents the basis of an extension field of Galois Field (GF) $GF(p^{M_T})$ over the base field, i.e., $GF(p)$. The vector associated with these fields is generalized as [44], [46]:

$$r_j = \beta_{1j}m_1 + \beta_{2j}m_2 + \beta_{3j}m_3 + \ldots + \beta_{M_Tj}m_{M_T} \tag{8}$$

where $\beta_{ij} \in GF(p)$.

In matrix notation, the vector r_j takes the form [44], [46]:

$$G_m(r) = \begin{bmatrix} \beta_{1,1} & \beta_{1,2} & \cdots & \beta_{1,M_T} \\ \beta_{2,1} & \beta_{2,2} & \cdots & \beta_{2,M_T} \\ \vdots & \vdots & \ddots & \vdots \\ \beta_{M_T,1} & \beta_{M_T,2} & \cdots & \beta_{M_T,M_T} \end{bmatrix} \tag{9}$$

As a result, the rank of the matrix, $G_m(r)$, is the total number of linearly independent rows or columns (whichever is smaller). However, the rank distance d_r between two vectors a and b is defined as the rank of the difference $a - b$ [46],

$$d_r(a, b) = r(a - b|p) \tag{10}$$

Based on the above equation (Eq. 10), the rank distance of a linear code $\mathcal{C}$ is given as:

$$d(\mathcal{C}) = min\{d_r(a, b)|a \in \mathcal{C}, b \in \mathcal{C}, a \neq b\} \tag{11}$$

If a linear code $\mathcal{C}$ has rank distance d, then all the errors e can be corrected [44]:

$$r(e|p) \leq t = \left\lfloor \frac{d-1}{2} \right\rfloor \tag{12}$$

Finally, there exists two possible types of rank codes which are described as:

(1) **Linear Rank codes for $n \leq M_T$**: A rank code can be defined as a linear code if the singleton-type bound, i.e., $k \leq n - d + 1$ is reached [47]. Such a code is considered to be an optimal code and its complete theoretical details can be found in [43]. For $n \leq M_T$, an optimal code exists only if $1 \leq d \leq n$ is satisfied and for such codes, a generator matrix can be realized as [47]:

$$G = \begin{bmatrix} \mathfrak{g}_1 & \mathfrak{g}_2 & \cdots & \mathfrak{g}_n \\ \mathfrak{g}_1^{[1]} & \mathfrak{g}_2^{[1]} & \cdots & \mathfrak{g}_n^{[1]} \\ \mathfrak{g}_1^{[2]} & \mathfrak{g}_2^{[2]} & \cdots & \mathfrak{g}_n^{[2]} \\ \vdots & \vdots & \ddots & \vdots \\ \mathfrak{g}_1^{[k-1]} & \mathfrak{g}_2^{[k1]} & \cdots & \mathfrak{g}_n^{[k-1]} \end{bmatrix} \tag{13}$$

where $\mathfrak{g}_1, \mathfrak{g}_2, \ldots, \mathfrak{g}_n$ denotes the set of elements that lies in the extension field $\mathbb{F}_{p^{M_T}}$. It is worth-noting here that these elements are also linearly independent. The aforesaid generator matrix Eq. 13 is also termed as Frobenius matrix [47]. In order to find out the code word c, consider an information vector $\mathbf{u} = (u_1, u_2, \cdots, u_k)$ of dimension k. The resultant code vector having dimension n is given as:

$$c\,(u) = uG \tag{14}$$

At receiver, $y = c(u) + e$ is received. To extract message information from vector y, the following condition should be satisfied:

$$GH^T = 0 \tag{15}$$

where H is referred to as parity check matrix and $(.)^T$ shows the transpose of the matrix. It is important to discuss here that an optimal rank code depends upon the following design parameters which are:

- Dimension: $k = n - d + 1$
- code word length: $n \leq M_T$
- Rank distance: $d = n - k + 1$

(2) **Linear Rank codes for $n > M_T$**: For $n > M_T$, the generator matrix given in Eq. 13 cannot generate a linear optimal code because the coordinates of generator vector are linearly dependent over $\mathbb{F}_p$. So, another type of rank codes is introduced by Gabidulin which is termed as reducible rank codes. This type of rank codes is a complete generalization of the rank product codes. The complete details of reducible rank codes can be found in [48]–[50]. Consider generator matrices $(G_1, G_2, \cdots, G_r)$ of linear codes (n_i, k_i) over the field $\mathbb{F}_{p^{M_T}}$, where $i = 1, 2, \cdots, p$. A rank code is said to be reducible if the generator matrix is given as [49]:

$$G = \begin{bmatrix} G_1 & 0 & 0 & \cdots & 0 & 0 \\ G_{21} & G_2 & 0 & \cdots & 0 & 0 \\ G_{31} & G_{32} & G_3 & \cdots & 0 & 0 \\ \vdots & \vdots & \vdots & \ddots & \vdots & \vdots \\ G_{p-1,1} & G_{p-1,2} & G_{p-1,3} & \cdots & G_{p-1} & 0 \\ G_{p,1} & G_{p,2} & G_{p,3} & \cdots & G_{p,p-1} & G_p \end{bmatrix} \tag{16}$$

Like optimal rank codes, a parity check matrix H is also required for decoding purpose. As the scope of this work is confined to evaluate the performance comparison of modified STBC with MRD based STBC so we only consider the first type ($n \leq M_T$) of rank codes. The next subsection discusses the construction of such codes.

1) CONSTRUCTION OF MRD-STBC

As the overall performance of STBCs depends upon the diversity gain which appears as one of the requirements for STBC construction by Tarokh *et al.* [51]. Likewise, diversity is also directly linked to the minimum rank distance between two codeword matrices. Therefore, the relationship between diversity gain and minimum rank distance (as well as the fact that two dimension MRD codes can be constructed) [43], results in applying MRD codes as STBC's. This is due to the fact that in a two dimensional MRD code, one dimension refers to transmit antennas and the other to distinct time-slots.

As discussed earlier, MRD codes are constructed using primitive polynomials. So, we consider a generic primitive polynomial of degree M_T such that,

$$f(y) = y^{M_T} + S_{M_T-1}y^{M_T-1} + S_{M_T-2}y^{M_T-2} + \ldots + S_0 \tag{17}$$

The companion matrix of dimension $(M_T \times M_T)$ can be formed using the above polynomial (Eq. 17) as follows [52]:

$$CM = \begin{bmatrix} 0 & 1 & 0 & \cdots & 0 & 0 \\ 0 & 0 & 1 & \cdots & 0 & 0 \\ 0 & 0 & 0 & \cdots & 0 & 0 \\ \vdots & \vdots & \vdots & \ddots & \vdots & \vdots \\ 0 & 0 & 0 & \cdots & 0 & 1 \\ S_0 & S_1 & S_2 & \cdots & S_{M_{T-2}} & S_{M_{T-1}} \end{bmatrix} \quad (18)$$

The set of possible rank codes can be obtained by multiplication operation. The successive multiplication of a companion matrix with itself would yield $(CM, CM^1, CM^2, \cdots, CM^{p^{M_T}-1})$. Depending on the value of M_T, the corresponding $GF(p^{M_T})$ is employed to design the companion matrices. Each row in the companion matrix consists of a primitive polynomial that represents a unique element of $GF(p^{M_T})$. For example, consider the construction of MRD-STBC for two transmit antennas. Consider y^2+y+1 as a primitive polynomial over $GF(2)$. According to the polynomial, the block size for MRD code is 4 and the direct matrix construction to create these 4 MRD blocks using Eq. 18 can be seen in [46]. These 4 MRD blocks are given as:

$$\begin{bmatrix} 0 & 0 \\ 0 & 0 \end{bmatrix}, \begin{bmatrix} 0 & 1 \\ 1 & 1 \end{bmatrix}, \begin{bmatrix} 1 & 1 \\ 1 & 0 \end{bmatrix}, \begin{bmatrix} 1 & 0 \\ 0 & 1 \end{bmatrix}$$

The above blocks show that they achieve full diversity gain since the number of time-slots is equivalent to symbols. Likewise, for any number of transmit antenna (M_T), the resultant companion matrix always attains full rate diversity gain which is not possible in OSTBC [51], [53]. This additional feature of MRD-STBCs can be satisfied by the construction of rank codes for four antennas. Consider a primitive polynomial of degree 4 which can be provided as $y^4 + y^3 + \beta y^2 + \beta y + \beta$, where the coefficients of the given polynomial are from $GF(2^2)$. The companion matrices of degree 4 using Eq. 18 can be formulated as [45]:

$$CM^1 = \begin{bmatrix} 0 & 0 & 0 & 0 \\ 0 & 0 & 0 & 0 \\ 0 & 0 & 0 & 0 \\ 0 & 0 & 0 & 0 \end{bmatrix},$$

$$CM^2 = \begin{bmatrix} 0 & 0 & 0 & \beta \\ 1 & 0 & 0 & \beta \\ 0 & 1 & 0 & \beta \\ 0 & 0 & 1 & \beta \end{bmatrix},$$

$$CM^3 = \begin{bmatrix} 0 & 0 & \beta & \beta \\ 0 & 0 & \beta & 0 \\ 1 & 0 & \beta & 0 \\ 0 & 1 & 1 & \beta^2 \end{bmatrix},$$

$$CM^{255} = \begin{bmatrix} 1 & 1 & 0 & 0 \\ 1 & 0 & 1 & 0 \\ \beta^2 & 0 & 0 & 1 \\ \beta^2 & 0 & 0 & 0 \end{bmatrix},$$

$$\vdots \qquad \vdots$$

$$CM^{256} = \begin{bmatrix} 1 & 0 & 0 & 0 \\ 0 & 1 & 0 & 0 \\ 0 & 0 & 1 & 0 \\ 0 & 0 & 0 & 1 \end{bmatrix}$$

It is pertinent to discuss here that each one of the above matrices are yield with the help of finite fields that are easily accessible in MATLAB. The resultant blocks for two or four transmitters are directly used to transmit from LEDs and these blocks can easily drive the LED driver circuit (ON/OFF) without any required modification, contrary to STBC which does require BPSK to OOK mapper to drive LEDs [31].

IV. NUMERICAL RESULTS

The current section exhibits an extensive assessment of the numerical results for the MIMO techniques introduced in section III. The computer based numerical simulations are conducted on the MATLAB tool. The overall performance of the proposed and existing MIMO systems are investigated and assessed with the help of E_b/N_o and BER based waterfall curves. In order to perform STBC coding, a modified STBC and MRD-STBCs is considered with one and two receiver(s). For each MIMO technique, 100,000 bits were generated randomly. The additional parameters required for the simulations of VLC channel and MIMO systems are listed in Table 1.

TABLE 1. Simulation parameters for VLC channel and MIMO systems.

Parameters	Values
Bits	10^5
Electrical Baseband Modulation	BPSK and OOK
Channel	LOS Optical Channel
Room dimensions	$4m \times 4m \times 3m$
Illuminance angle ϕ	5° - 15°
Semi-angle at half power $(\varphi_{1/2})$	15°
Receiver's FOV	15°
Photo-detector area	$1\ cm^2$
Responsitivity	1
SNR	$0 - 26$ dB
Noise	AWGN
Receiver	Zero-forcing

A. SIMULATION SETUP

For numerical simulations, various LOS configurations are considered by changing the spacing between transmitters. To make the evaluation procedure fair, the average optical power emitted by the transmitters for each MIMO technique is uniform. The error performance at the receiver side is evaluated with respect to bit energy to noise power spectral density (E_b/N_o) and we take under consideration the specific path-loss of every setup because of the angular placement and distance between the single emitter and receiver. Additionally, the response of the optical channel remains stable during the transmission of each block code. Furthermore, AWGN sources are also considered at the receiving photo-diodes.

On the receiver side, the block codes are acquired which are corrupted due to channel impairments and noise. These block codes are passed to the zero-forcing (ZF) detector. Although,

it is found in the literature that ML detector outperforms the ZF, yet it is not suitable for physical implementation as by increasing the constellation points or by transmitting antennas the number of block code combinations increases, ultimately, results in computational inefficiency. Therefore, a ZF linear detector is used in this work that reduces the computational complexity and becomes a viable solution in physical implementation.

B. NUMERICAL RESULTS AND DISCUSSION ON CHANNEL MATRICES

For simulations, we consider two configurations (2×1 and 2×2) with two distinct transmitter spacings M_{T_s}. The spacing between the receivers is fixed while the transmitter spacings are selected as $M_{T_s} = 0.25$, and $0.5m$ respectively. Moreover, the spacing between the LEDs in an array is kept constant. This means that the channel matrices depends only on the alignment of transmitters and receivers. By using Eq. 3 and the room dimensions given in section II, the channel matrices without noise are as follows:

$$H_{M_{T_s}=0.25} = 10^{-3}\begin{bmatrix} 0.1261 & 0.1085 \\ 0.1085 & 0.1261 \end{bmatrix},$$
$$H_{M_{T_s}=0.75} = 10^{-3}\begin{bmatrix} 0.1063 & 0.0771 \\ 0.0771 & 0.1063 \end{bmatrix} \quad (19)$$

The above channel matrices lead us to a crucial point i.e., for LOS scenario, the symmetrical placement of VLC transmitters and receivers provide us equal channel gains. Furthermore, it can also be deduced from the aforementioned matrices that if the spacing between the transmitters are kept small then we get similar channel gains, however, if the spacing is large then the channel gains are no longer similar. By simulating the MATLAB code for the channel matrices, it is observed that when the spacing between the transmitters is 0.55m, the transmitter is not in the range of FOV of the receiver, thus the particular transfer factor $h_{M_R M_T}$ is equal to zero.

C. NUMERICAL RESULTS AND DISCUSSION ON 2 × 1 CONFIGURATION

For 2×1 configuration, the BER results for RC, SMP, MSTBC and MRD-STBCs are shown in Fig. 3. For transmitters spacing $0.25m$, it is noticeable from the results that at BER $= 10^{-3}$, the RC outperform all other MIMO techniques. The RC achieves a coding gain of approximately 5 and 7 dB when compared to the STBCs and SMP. This significant improvement in RC is due to the light intensities from different transmitters are constructively gathered at the single receiver. Similar results are also reported in [24], [31], [34]. A very interesting result can be observed for STBC. Although, STBC perform worse than the RC but attains a gain of 2 dB in comparison with SMP. Moreover, both STBCs (MSTBC and MRD-STBC) perform exactly same. This means that the suggested MRD-STBC become a good alternative to MSTBC as it does not require any mapping block that converts a BPSK signal into OOK.

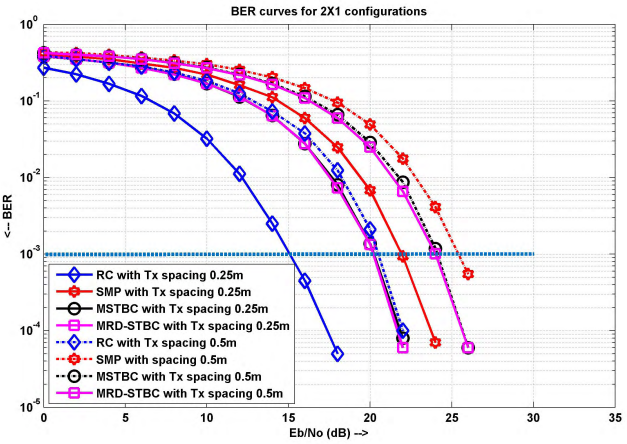

FIGURE 3. Error performance of different MIMO techniques for 2 × 1 configuration.

The results for transmitter spacing $0.5m$ are also shown in Fig. 3. The results show that by expanding the spacing between the transmitters, the error results for all MIMO techniques deteriorate and thus require additional E_b/N_o to attain a fixed BER. This performance deterioration is due to the fact that the light intensities decrease as VLC transmitters move away from each other. At BER $= 10^{-3}$, the performance of RC is 5.1 dB worse than the RC at spacing $0.25m$. Consequently, the performance of STBCs also become worse and require an additional E_b/N_o of 3.9 dB to get fixed BER. The similar result can also be observed for SMP as it requires 3.7 dB more E_b/N_o.

D. NUMERICAL RESULTS AND DISCUSSION ON 2 × 2 CONFIGURATION

This subsection illustrates the BER performance results of all MIMO techniques for 2×2 configurations. The simulation setup is similar to the 2×1 configuration instead another VLC receiver is added and aligned at the spacing of $0.1m$. Fig. 4 demonstrates the BER results of all MIMO techniques

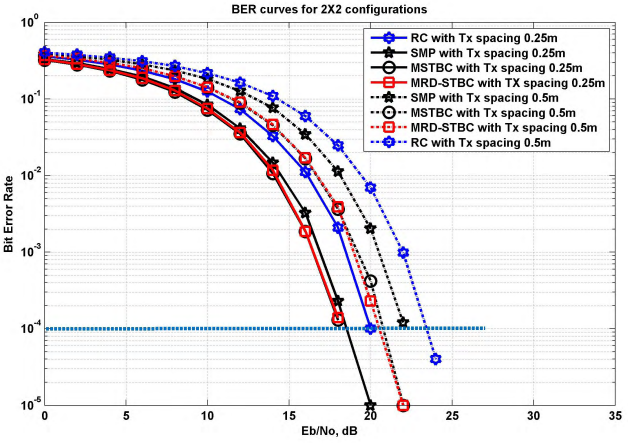

FIGURE 4. Error performance of different MIMO techniques for 2 × 2 configuration.

with different transmitters spacing. From the results, at BER $= 10^{-4}$ and spacing $0.25m$, STBCs and SMP performed better than the RC. This performance improvement occurs at the expense of extra complexity at the receiver side. Like 2×1 configuration, the performance of both STBCs (MSTBC and MRD-STBC) is exactly the same and achieves a coding gain of about 2 and 0.3 dB with respect to RC and SMP respectively. Moreover, the SMP with its multiplexing gain outperform RC and requires 1.7 dB less E_b/N_o. The similar trend is also noticed from the simulation outcomes at the transmitters spacing $0.5m$. To attain BER $= 10^{-4}$, STBCs require 3 dB extra E_b/N_o in comparison to the STBCs at $0.25m$ spacing while SMP and RC both require 3.7 dB E_b/N_o.

V. EXPERIMENTAL SETUP

This section demonstrates the hardware design of a complete state of the art MIMO-VLC transceiver. The SDR is created using LabVIEW tool in which MIMO techniques are implemented to transmit/receive data through an optical wireless channel [54]. For real-time text transmission, NI cDAQ 9174 chassis fixed with ADC and DAC modules, is used [55]. The output of the SDR is connected to NI 9263 analog output module which acts as DAC [56]. It is a screw terminal connector module that has 4 output channels. The LED driving circuit can be connected to any one of these channels. The input to SDR is received from the NI 9201 analog input module connected with the output of the photo-diodes and it has 8 input channels [57]. The complete hardware setup is shown in Fig. 5 while some important features of all hardware equipment are given in Table 2. It is worth-noting here that the transmitters and receivers employed in this work are different from those used in our earlier work [23]. This change is due to the bottleneck of the photo-diode (OPT101) as it is not able to detect optical signals greater than 4 KHz. Hence, it also restricts the final data-rate of the VLC system. The transmitters and receivers used in this work are discussed in forthcoming subsections.

A. VLC TRANSMITTER

In a VLC system, the optical transmitter (LEDs) is employed to transform the electrical signals into light. It comprises

TABLE 2. Features of hardware equipment.

Hardware Equipment	Specifications	Description
NI 9201 Input module	Channels	8 analogue input channels
	Sample rate	$500\ KS/s$
	ADC resolution	12 bits
NI 9263 Output module	Channels	4 analogue output channels
	Sample rate	$100\ KS/s$
	DAC resolution	16 bits
LED (LXHL-BM01)	Operational life	$100\ K$ hours
	Radiation pattern	Bat-wing
	Viewing Angle	110°
	Switching Speed	$100\ ns$
Photo-diode (BPW34)	Area	$7.5\ mm^2$
	Response time	$10\ ns$
	Sensitivity angle	65°

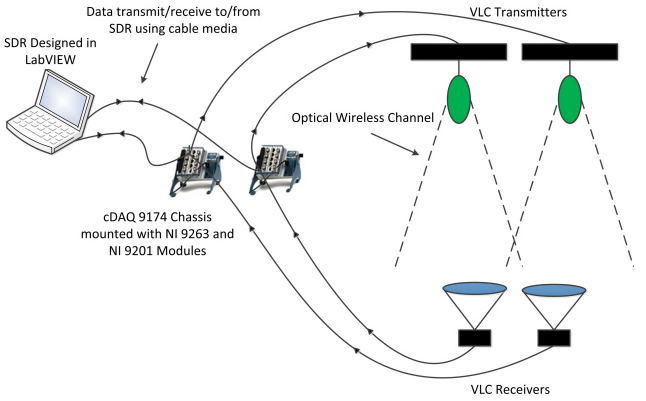

FIGURE 5. Hardware setup of MIMO-VLC system.

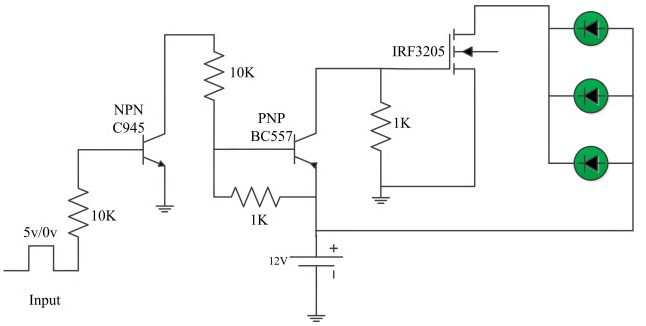

FIGURE 6. VLC transmitter used for prototype.

an LED driver circuit and LEDs that can perform the dual operation (illumination and data communication). The LED driver circuit needs a $12v$ DC supply that is sufficient to operate 3 LEDs that we have used in our set up. These 3 LEDs are connected such that the input voltage is divided across each LED [39]. The LEDs selected for the prototype are *LXHL-BM01* and they have high switching capability such that their flickering time (light ON and OFF) is 100 ns [58]. The complete VLC transmitter is shown in Fig. 6.

B. VLC RECEIVER

The VLC receiver comprises photo-diodes and an amplification circuit. The photo-diode used for the prototype design is $BPW34$. It is a silicon PIN photo-diode that is highly susceptible to infrared and visible radiation. The motivation behind the selection of $BPW34$ photo-diode is its high photo and radiant sensitivity and faster response time. These attributes make it an ideal choice to gather light intensity at a wider angle [59]. The detected optical signal is first converted to an electrical signal. Since the output voltage from the photo-diode is very low, the desired voltage level ($+5v$ or $0v$) is achieved by passing the signal through an amplifier circuit. For this reason, the $LM358$ IC is employed as an amplifier. The schematic diagram of an amplifier circuit is shown in Fig. 7. This circuit is developed in such a way that the sensitivity of the photo-diode to fluorescent light is reduced. This is done with the help of $10\ K\Omega$ variable resistor. By setting the value on variable resistor VR_2, the photo-diode

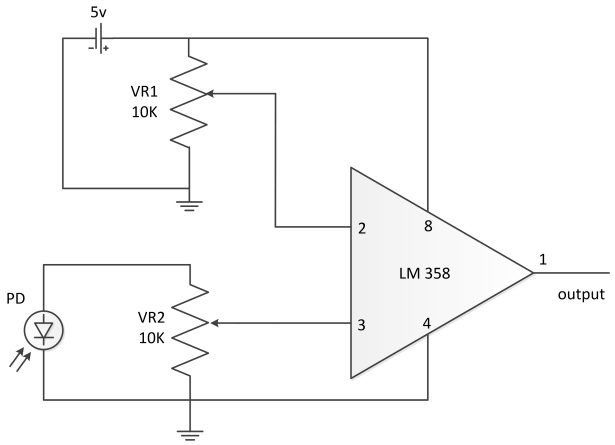

FIGURE 7. VLC receiver used for prototype.

only detects the light from the transmitter. The output of the amplifier is then input to cDAQ module.

C. SOFTWARE DEFINED RADIO

The modem for MIMO techniques is designed in LabVIEW. For 2×2 MIMO configuration, two separate I/O physical channels are required each for a single VLC transmitter/receiver while for 2×1 only one input physical channel is required. For text transmission, the payload comprises 16 characters. These characters are then converted to bits and passed to MATLAB script library where OOK modulation is done. As data is transmitted by two VLC transmitters simultaneously, the modulated signal is divided into two equal parts. The data is then mapped onto RC, SMP, MSTBC and MRD-STBC blocks and an array of $1's$ are added. The complete block diagram of MIMO-VLC SDR is demonstrated in Fig. 8.

The final output of all schemes directly leads to the physical layer by using two separate NI 9263 modules. The optical signals are received by *BPW*34 photo-diodes and amplified using amplification circuit as discussed earlier. These signals are corrupted due to channel effects and the light from fluorescent lamps available in indoor environment. To recover the transmitted signals, ZF detection is performed.

The next implementation step is to apply synchronization operation which is necessary due to early or delayed detection of the signal [23], [39]. For synchronization, the receiver must have the knowledge of added $1's$. The cross-correlation operation is carried out between the range of inserted $1's$ and estimated data which results in original data. When the number of $1's$ starts overlapping with the $1's$ that are inserted with the original data, the outcome of correlation continues on increasing and reaches to its highest value at the time when the window of $1's$ is completely overlapped with the inserted $1's$. The data after the window is our message and it is passed to demapper where original symbols are separated from blocks. These symbols are then combined to form a single OOK symbol.

D. EXPERIMENTAL RESULTS, DATA-RATE AND TRANSMISSION RANGE OF THE PROTOTYPE

Fig. 9 exhibits the virtual instruments (VI) diagram of MIMO techniques based VLC prototype. A message of 16 characters is transmitted by the prototype. After necessary conversion, the message bits are 128 in length and to make it round off, two dummy bits are added. Hence, the complete message bits carried by two symbols are 130 [23]. In an event where the user writes nothing in the message space then the prototype sends ASCII value of 16 spaces. Since 2 VLC transmitters are used to transmit the OOK symbol, so the original signal is divided into two equal parts and mapped onto the RC, STBC, and SMP blocks. In RC, the OOK symbols are carried in the first time-slot while the same symbols are transmitted in the second time-slot. Similarly, in STBC the complex conjugates of symbols s_1 and s_2 are transmitted in the second time-slot. Both RC and STBCs are used to increase the reliability of the VLC system. In an effort to maximize the capacity, SMP is used in which two different symbols are transported in every time-slot. Hence, the data-rate of the prototype is double. After mapping, the cyclic suffix will be appended with the data. The cyclic suffix is very helpful for the receiver mainly because at the time of synchronization if any sample is misplaced it will eventually make no difference in the operation, as the misplaced sample is just the sample of cyclic suffix [21], [23], [39]. After the add-on of cyclic suffix bits, the overall size of each bit-stream for RC/STBC and SMP are 170 and 105 bits.

To represent the start of the symbol, 40 ones are padded before the bit-streams that are transmitted from two VLC transmitters. This makes the total symbol length of 210 and 145 bits respectively. These bit-streams are converted to an analog signal and transmitted through two NI 9263 units at the transmission speed of 15 *kbps* and acquired at similar speed by NI 9201 units. This bit rate would result in 71.429 RC/STBC $symbols/s$ and 103.449 SMP $symbols/second$. Therefore, the final data-rate of the RC/STBC based MIMO system is 9.2857 *Kbps* while using SMP, the data-rate is 15 *Kbps*.

It is worthy to state that the developed MIMO system has hardware constraint in terms of transmission and reception rate. When we increase the transmission rate over 15 *KHz*, the modules are no longer synchronized with each other. Also, the above reported data-rates (9.2857 & 15 *Kbps*) are very low and this is due to the usage of baseband modules (NI cDAQ). In the future, we intend to use broadband modules like Universal Software Radio Peripheral (USRP) or Field Programmable Gate Array (FPGA) kits to boost the spectral efficiency.

To find the range of MIMO prototype, the experiments are conducted for two configurations (2×1 and 2×2) in a brightly lit room. As stated in section II, the spacing between the transmitters and receivers are set to be $0.25m$ and $0.1m$ respectively. The experiments for 2×1 configuration exhibits that RC gives an error-free text transmission at the range of

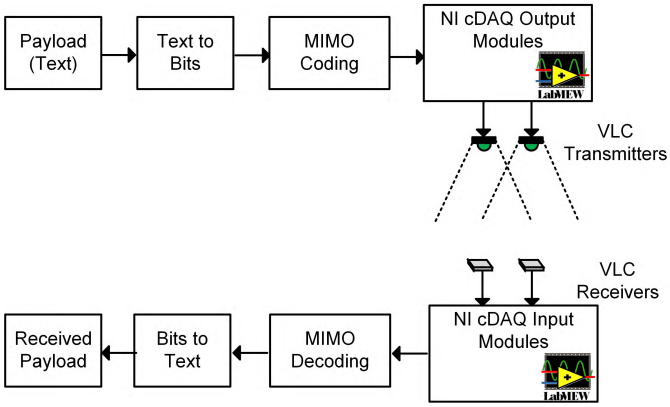

FIGURE 8. Block diagram of MIMO-VLC SDR.

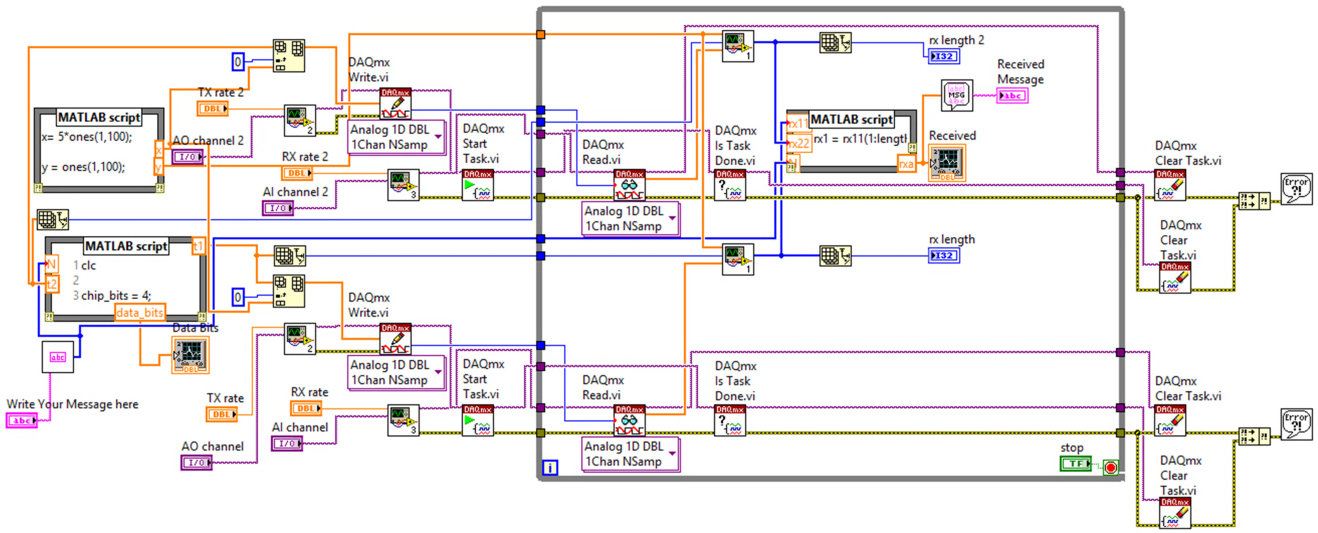

FIGURE 9. VI of MIMO-VLC prototype.

1.45m and outperform all MIMO techniques. On the other hand, STBCs provides errorless communication up to 1.18m while the range for SMP is limited to 1.09m. It is also noted from the experiment results that above 1.45m the errors occur in RC based MIMO scheme and these errors continuously increasing with the increase in transmission range. At 1.77m, the receiver lost the signal and nothing is received at the output. The similar results are observed for STBCs and SMP, however, the only variation observed is the enhancement in the range. Both STBCs (MSTBC & MRD-STBC) gathered the signal up to 1.33m. Above this range, the signal is lost while the transmission range of SMP is limited to the only 1.17m. The experimental results for both configurations on transmission range are listed in Table 3.

The experiments were also conducted for 2 × 2 configurations while keeping the spacing constant. The outcome of experiments reveals that the performance of RC becomes worst by introducing a receiver. The transmission range for RC based 2 × 2 configurations are limited to 1.46m. Above this range, the receiver lost the signal. However, by adding another receiver, the reliability of the STBC based VLC system is improved and the errorless communication is done at 1.43m. If we increase the distance beyond this range than errors occur and after 1.59m the signal is lost. The transmission range for SMP is also enhanced as it takes the full advantage of multiplexing gain. The error-free communication with SMP has occurred at the range of 1.41m and

TABLE 3. Experimental results on transmission range.

MIMO-VLC System	Configurations	Transmission Range	Signal Lost Range
RC	2 × 1	1.45 m	1.77 m
	2 × 2	1.29 m	1.46 m
MRD-STBCs	2 × 1	1.18 m	1.33 m
	2 × 2	1.43 m	1.59 m
SMP	2 × 1	1.09 m	1.17 m
	2 × 2	1.41 m	1.56 m

above 1.56m receiver receives nothing at the output. From the hardware-based numerical results of both configurations, a very crucial fact can be deduced that if we want to exploit the transmit diversity then we must select RC for VLC system as it provides the maximum transmission range. Moreover, if we are dealt with the high data-rate transmission, then SMP is the best option.

VI. CONCLUSION

The current work includes both simulation and hardware-based comparative analysis of different MIMO techniques for indoor VLC environment. The VLC transceiver prototype has been developed using NI equipment whereas simulations are conducted using MATLAB tool. For analysis, two configurations (2×1 & 2×2) with different transmitters spacing are considered while keeping the receiver spacing fixed. It has been shown in both simulations and experimentation that the RC for 2×1 configuration provides a significant amount of diversity gain and outperform all other MIMO schemes. This performance enhancement is the result of non-negativity of the channel gains that ensure the nondestructive interference at the receiver. The error-free range provided by the RC is 1.45m which is larger than any another MIMO scheme. However, by the addition of receiver in the setup, the performance of RC becomes worst. For 2×2 configurations, STBCs performed better than RC and SMP. The experimental results showed that STBCs achieve an error-free range of 1.43m which is better than 2×2 RC and SMP. Finally, for high data rate applications, we can utilize SMP as a MIMO technique. On the other hand, if we need to transmit the information at longer range then we can adopt RC or STBC depending on the configuration. The future work may include the implementation of MRD-STBC based VLC transceiver on advanced modules like USRP or FPGA's that can boost the data-rate up to *Mbps*.

REFERENCES

[1] T. Komine and M. Nakagawa, "Fundamental analysis for visible-light communication system using LED lights," *IEEE Trans. Consum. Electron.*, vol. 50, no. 1, pp. 100–107, Feb. 2004.
[2] N. Chi, H. Haas, M. Kavehrad, T. D. C. Little, and X.-L. Huang, "Visible light communications: Demand factors, benefits and opportunities," *IEEE Wireless Commun.*, vol. 22, no. 2, pp. 5–7, Apr. 2015.
[3] L. U. Khan, "Visible light communication: Applications, architecture, standardization and research challenges," *Digit. Commun. Netw.*, vol. 3, no. 2, pp. 78–88, May 2016.
[4] S. Rajagopal, R. D. Roberts, and S.-K. Lim, "IEEE 802.15.7 visible light communication: Modulation schemes and dimming support," *IEEE Commun. Mag.*, vol. 50, no. 3, pp. 72–82, Mar. 2012.
[5] Z. Zhou, J. Feng, B. Gu, B. Ai, S. Mumtaz, J. Rodriguez, and M. Guizani, "When mobile crowd sensing meets UAV: Energy-efficient task assignment and route planning," *IEEE Trans. Commun.*, vol. 66, no. 11, pp. 5526–5538, Nov. 2018.
[6] A. Jovicic, J. Li, and T. Richardson, "Visible light communication: Opportunities, challenges and the path to market," *IEEE Commun. Mag.*, vol. 51, no. 12, pp. 26–32, Dec. 2013.
[7] L. Garber, "Turning on the lights for wireless communications," *Computer*, vol. 44, no. 11, pp. 11–14, 2011.
[8] C.-W. Chow, C.-H. Yeh, Y. Liu, C.-W. Hsu, and J.-Y. Sung, "Network architecture of bidirectional visible light communication and passive optical network," *IEEE Photon. J.*, vol. 8, no. 3, Jun. 2016, Art. no. 7904506.
[9] W. Ye, J. Chen, B. Lin, X. Tang, and Z. Ghassemlooy, "Experimental demonstration of bidirectional IDMA for visible light communication," in *Proc. Opto-Electron. Commun. Conf. (OECC) Photon. Global Conf. (PGC)*, Jul. 2017, pp. 1–3.
[10] G. Cossu, R. Corsini, and E. Ciaramella, "High-speed bi-directional optical wireless system in non-directed line-of-sight configuration," *J. Lightw. Technol.*, vol. 32, no. 10, pp. 2035–2040, May 15, 2014.
[11] K. Choi, Y. Jang, J. Noh, M. Ju, and Y. Park, "Visible light communications with color and dimming control by employing VPPM coding," in *Proc. 4th Int. Conf. Ubiquitous Future Netw. (ICUFN)*, Jul. 2012, pp. 10–12.
[12] X. Liu, A. Yang, Y. Li, and L. Feng, "Separate dimming controlling and data transmission for an indoor visible light communication system," *China Commun.*, vol. 12, no. 3, pp. 71–76, 2015.
[13] K. Lee and H. Park, "Modulations for visible light communications with dimming control," *IEEE Photon. Technol. Lett.*, vol. 23, no. 16, pp. 1136–1138, Aug. 15, 2011.
[14] H. Elgala, R. Mesleh, and H. Haas, "Practical considerations for indoor wireless optical system implementation using OFDM," in *Proc. 10th Int. Conf. Telecommun. (ConTEL)*, Jun. 2009, pp. 25–29.
[15] J. Armstrong, "OFDM for optical communications," *J. Lightw. Technol.*, vol. 27, no. 3, pp. 189–204, Feb. 1, 2009. [Online]. Available: http://jlt.osa.org/abstract.cfm?URI=jlt-27-3-189
[16] S. D. Dissanayake and J. Armstrong, "Comparison of ACO-OFDM, DCO-OFDM and ADO-OFDM in IM/DD systems," *J. Lightw. Technol.*, vol. 31, no. 7, pp. 1063–1072, Apr. 1, 2013.
[17] J. Dang, Z. Zhang, and L. Wu, "A Novel Receiver for ACO-OFDM in Visible Light Communication," *IEEE Commun. Lett.*, vol. 17, no. 12, pp. 2320–2323, Dec. 2013.
[18] M. Zhang and Z. Zhang, "An optimum DC-biasing for DCO-OFDM system," *IEEE Commun. Lett.*, vol. 18, no. 8, pp. 1351–1354, Aug. 2014.
[19] W. Zhong, C. Chen, and D. Wu, "Non-hermitian symmetry OFDM for indoor space division multiplexing visible light communications," in *Proc. 18th Int. Conf. Transparent Opt. Netw. (ICTON)*, Jul. 2016, pp. 1–4.
[20] N. Bahra and G. A. Hodtani, "A modified SLM technique for PAPR reduction in OFDM systems by using a novel phase sequence," *Int. J. Electron. Lett.*, vol. 6, no. 1, pp. 90–97, 2018.
[21] M. Ahsan and H. M. Asif, "ESIM-OFDM-based transceiver design of a visible light communication system," *Int. J. Commun. Syst.*, vol. 30, no. 8, p. e3175, 2017.
[22] Z. Yu, A. J. Redfern, and G. T. Zhou, "Using delta-sigma modulators in visible light OFDM systems," in *Proc. 23rd Wireless Opt. Commun. Conf. (WOCC)*, May 2014, pp. 1–5.
[23] A. Khalid and H. M. Asif, "OCDMA and OSTBC based VLC transceiver design using NI cDAQ," *Photon. Netw. Commun.*, vol. 35, no. 1, pp. 97–108, 2018.
[24] A. Alwarafy, M. Alresheedi, A. F. Abas, and A. Alsanie, "Performance evaluation of space time coding techniques for indoor visible light communication systems," in *Proc. Int. Conf. Opt. Netw. Design Modeling (ONDM)*, May 2018, pp. 88–93.
[25] M. Biagi, A. M. Vegni, S. Pergoloni, P. M. Butala, and T. D. C. Little, "Trace-orthogonal PPM-space time block coding under rate constraints for visible light communication," *J. Lightw. Technol.*, vol. 33, no. 2, pp. 481–494, Jan. 15, 2015.
[26] X.-C. Gao, J.-K. Zhang, and J. Jin, "Linear space codes for indoor MIMO visible light communications with ML detection," in *Proc. 10th Int. Conf. Commun. Netw. China (ChinaCom)*, Aug. 2015, pp. 142–147.
[27] M. Biagi and A. M. Vegni, "Enabling high data rate VLC via MIMO-LEDs PPM," in *Proc. IEEE Globecom Workshops (GC Wkshps)*, Dec. 2013, pp. 1058–1063.
[28] C. He, T. Q. Wang, and J. Armstrong, "Performance comparison between spatial multiplexing and spatial modulation in indoor MIMO visible light communication systems," in *Proc. Int. Conf. Commun. (ICC)*, May 2016, pp. 1–6.
[29] L. Zeng, D. C. O'Brien, H. Le Minh, G. E. Faulkner, K. Lee, D. Jung, Y. Oh, and E. T. Won, "High data rate multiple input multiple output (MIMO) optical wireless communications using white LED lighting," *IEEE J. Sel. Areas Commun.*, vol. 27, no. 9, pp. 1654–1662, Dec. 2009.
[30] Y.-J. Zhu, Z.-G. Sun, J.-K. Zhang, Y.-Y. Zhang, and J. Zhang, "Training receivers for repetition-coded MISO outdoor visible light communications," *IEEE Trans. Veh. Technol.*, vol. 66, no. 1, pp. 529–540, Jan. 2017.
[31] M. Safari and M. Uysal, "Do we really need OSTBCs for free-space optical communication with direct detection?" *IEEE Trans. Wireless Commun.*, vol. 7, no. 11, pp. 4445–4448, Nov. 2008.

[32] T. Fath and H. Haas, "Performance comparison of MIMO techniques for optical wireless communications in indoor environments," *IEEE Trans. Commun.*, vol. 61, no. 2, pp. 733–742, Feb. 2013.
[33] E. J. Lee and V. W. S. Chan, "Part 1: Optical communication over the clear turbulent atmospheric channel using diversity," *IEEE J. Sel. Areas Commun.*, vol. 22, no. 9, pp. 1896–1906, Nov. 2004.
[34] S. G. Wilson, M. Brandt-Pearce, Q. Cao, and M. Baedke, "Optical repetition MIMO transmission with multipulse PPM," *IEEE J. Sel. Areas Commun.*, vol. 23, no. 9, pp. 1901–1910, Sep. 2005.
[35] T. Ganjian, G. Baghersalimi, and Z. Ghassemlooy, "Performance evaluation of the received power based on the transmitter position in a visible light communications system," in *Proc. Iranian Conf. Electr. Eng. (ICEE)*, Tehran, Iran, May 2017, pp. 1763–1768. [Online]. Available: http://ieeexplore.ieee.org/document/7985336/
[36] C. Chen, D. Basnayaka, and H. Haas, "Non-line-of-sight channel impulse response characterisation in visible light communications," in *Proc. IEEE Int. Conf. Commun. (ICC)*, May 2016, pp. 1–6.
[37] A. Zafar, A. Khalid, and H. M. Asif, "Equalization techniques for visible light communication system," in *Proc. IEEE Int. Conf. Elect. Comput. Technol. Appl. (ICECTA)*, Nov. 2017, pp. 1–5. [Online]. Available: http://ieeexplore.ieee.org/document/8251941/
[38] J. M. Kahn and J. R. Barry, "Wireless infrared communications," *Proc. IEEE*, vol. 85, no. 2, pp. 265–298, Feb. 1997.
[39] A. Khalid, H. M. Asif, and Nesruminallah, "NI cDAQ based software-defined radio for visible light communication system," in *Proc. 2nd Workshop Recent Trends Telecommun. Res. (RTTR)*, Feb. 2017, pp. 1–5.
[40] C. Li, Y. Yi, K. Lee, and K. Lee, "Performance analysis of visible light communication using the STBC-OFDM technique for intelligent transportation systems," *Int. J. Electron.*, vol. 101, no. 8, pp. 1117–1133, 2014.
[41] O. Bouchet, G. Faulkner, L. Grobe, E. Gueutier, K. D. Langer, S. Nerreter, D. O'Brien, R. Turnbull, J. Vucic, J. W. Walewski, and M. Wolf, "Deliverable D4.2b physical layer design and specification," in *Proc. 7th Framework Programme Inf. Commun. Technol.*, 2011.
[42] C. Abou-Rjeily, "Diversity orders and coding gains of repetition coding and transmit laser selection over MIMO free-space optical links," in *Proc. 11th Int. Symp. Wireless Commun. Syst. (ISWCS)*, Aug. 2014, pp. 90–94.
[43] È. M. Gabidulin, "Theory of codes with maximum rank distance," *Problemy Peredachi Inform.*, vol. 21, no. 1, pp. 3–16, 1985.
[44] E. M. Gabidulin and N. I. Pilipchuk, "Error and erasure correcting algorithms for rank codes," *Des., Codes Cryptogr.*, vol. 49, no. 1, pp. 105–122, Dec. 2008.
[45] H. Asif, B. Honary, and M. T. Hamayun, "Gaussian integers and interleaved rank codes for space–time block codes," *Int. J. Commun. Syst.*, vol. 30, no. 1, p. e2943, 2017. [Online]. Available: http://onlinelibrary.wiley.com/doi/10.1002/dac.2943/full
[46] H. M. Asif, E. M. Gabidulin, and B. Honary, "Maximum rank distance codes for space time block coding: A comparative study," in *Proc. 5th Int. Conf. Next Gener. Mobile Appl., Services Technol. (NGMAST)*, Sep. 2011, pp. 206–211.
[47] H. Rashwan, È. M. Gabidulin, and B. Honary, "Security of the GPT cryptosystem and its applications to cryptography," *Secur. Commun. Netw.*, vol. 4, no. 8, pp. 937–946, 2011.
[48] U. Martínez-Peñas, "Generalized rank weights of reducible codes, optimal cases, and related properties," in *Proc. IEEE Int. Symp. Inf. Theory (ISIT)*, Sep. 2016, pp. 1959–1963.
[49] E. Khan, E. Gabidulin, B. Honary, and H. Ahmed, "Modified niederreiter type of GPT cryptosystem based on reducible rank codes," *Des., Codes Cryptogr.*, vol. 70, nos. 1–2, pp. 231–239, 2014.
[50] E. M. Gabidulin, A. Ourivski, B. Ammar, and B. Honary, "Reducible rank codes and applications to cryptography," in *Information, Coding and Mathematics*. Boston, MA, USA: Springer, 2002, pp. 121–132.
[51] V. Tarokh, N. Seshadri, and A. R. Calderbank, "Space-time codes for high data rate wireless communication: Performance criterion and code construction," *IEEE Trans. Inf. Theory*, vol. 44, no. 2, pp. 744–765, Mar. 1998.
[52] H. Bart, I. Gohberg, M. Kaashoek, and A. C. Ran, *Factorization of Matrix and Operator Functions: The State Space Method*, vol. 178. Springer, 2007.
[53] Y. S. Cho, J. Kim, W. Y. Yang, and C. G. Kang, *MIMO-OFDM Wireless Communications With MATLAB*. Hoboken, NJ, USA: Wiley, 2010.
[54] J. Wu, S. Luo, S. Wang, and H. Wang, "NLES: A novel lifetime extension scheme for safety-critical cyber-physical systems using SDN and NFV," *IEEE Internet Things J.*, vol. 6, no. 2, pp. 2463–2475, Apr. 2019.
[55] National Instruments. *NI 9174*. [Online]. Available: www.ni.com/pdf/manuals/374045a.pdf
[56] National Instruments. *NI 9263*. [Online]. Available: http://sine.ni.com/nips/cds/view/p/lang/en/nid/208806
[57] National Instruments. *NI 9201*. [Online]. Available: http://sine.ni.com/nips/cds/view/p/lang/en/nid/208798
[58] Lumileds Lighting. (2005). *Luxeon Emitter*. [Online]. Available: https://www.sparkfun.com/datasheets/Components/Luxeon-I.pdf
[59] Vishay Intertechnology. (Aug. 23, 2011). *Silicon Pin Photodiodes*. [Online]. Available: www.vishay.com/docs/81521/bpw34.pdf

ARSLAN KHALID received the B.S. and M.S. degrees in electrical engineering from the COMSATS Institute of Information Technology, Lahore, Pakistan, in 2012 and 2016, respectively. He is currently with the Department of Electrical Engineering, The University of Lahore, Pakistan, as a Lecturer. His research interests include communication theory, wireless communication systems, visible light communication, MIMO systems and its types, i.e., repetition coding, spatial multiplexing, space-time block codes, rank codes, and their applications, channel modeling, and software-defined radios.

HAFIZ M. ASIF received the B.S. degree in electrical engineering from UET, Lahore, Pakistan, in 2002, the M.S. degree in computer engineering from the King Fahad University of Petroleum and Minerals (KFUPM), in 2007, and the Ph.D. degree in communication systems from Lancaster University, U.K., in 2012. He is currently with the Department of Electrical Engineering, COMSATS Lahore, Pakistan. He is also with the Department of Electrical Engineering, Taif University (TU), Saudi Arabia. His research interests include visible light communication, space-time block codes, rank codes, wireless communication systems, and computer networks.

SHAHID MUMTAZ received the master's degree from the Blekinge Institute of Technology, Sweden, in 2006, and the Ph.D. degree in electrical and electronic engineering from the University of Aveiro, Portugal, in 2011. He has more than ten years of wireless industry and academic experience, and is currently a Principal Research Scientist and Technical Manager with the Instituto de Telecomunicações, Portugal. From 2005 to 2006, he was with Ericsson and Huawei at Research Labs, Sweden. Since 2015, he has been with the Department of Electronic and Electrical Engineering, University of Aveiro, Portugal, where he is currently an Assistance Professor and the Director of the Wireless Networking and Communications Group. He is also the CTO of two startups and SMEs in Portugal. His research interests include several aspects of wireless and vehicular communication. He uses mathematical and system level tools to model and analyze emerging wireless communication architectures, leading to innovative and theoretically optimal new communication techniques. He is working closely with leading research and development groups in the industry to transition these ideas to practice. His work is currently supported by Samsung, Huawei, and Ericsson, as well as Fundacao Ciencia e Tecnologia (FCT), Portugal.

SATTAM AL OTAIBI is the Head of the Innovation and Entrepreneurship Center, Taif University, Saudi Arabia. He is a researcher and an academician specializing in electrical engineering and nanotechnology. His practical experience in the field of industry, education, and scientific research has been formed through his research work and through his mobility among many companies, institutions, and universities as well as active participation in research centers that resulted in many scientific researches published in refereed scientific bodies.

KOSTROMITIN KONSTANTIN graduated (with Hons.) from the Municipal Secondary School, Chelaybinsk, and entered the Physical Department of Education, Chelaybinsk State University, with specialization in physics. He received the bachelor's and master's degrees in physics with specialization in chair physics of condensed matter from Chelyabinsk State University, in 2008 and 2010, respectively. He completed the Ph.D. thesis entitled ''Researching of Magnetocaloric Effect in Antiferromagnetics and Twins Moving in Heusler alloys'' with specialization in physics of condensed matter in the Dissertation Council of Chelyabinsk State University, in 2013.